

Early cytokine and chemokine signals shape the anti-AML activity of bispecific engager-secreting T cells

Natalie J. Holl,¹ Adam Fearnow,¹ Ilias Christodoulou,¹ Stamatia C. Vorri,¹ Ruyan Rahnama,¹ Jun Choe,¹ Alokesh Ghosal,² Weng-Ian Ng,² Vinay Vyas,² Hannah W. Song,³ Ravi Varadhan¹ and Challice L. Bonifant¹

¹Department of Oncology, Sidney Kimmel Comprehensive Cancer Center, Johns Hopkins University School of Medicine, Baltimore; ²Biopharmaceutical Development Program, Frederick National Laboratory for Cancer Research, Leidos Biomedical Research Inc., Frederick and ³Center for Cellular Engineering, Department of Transfusion Medicine, National Institutes of Health, Bethesda, MD, USA

Correspondence: C. L. Bonifant
cbonifa2@jh.edu

Received: March 31, 2025.
Accepted: August 29, 2025.
Early view: September 11, 2025.

<https://doi.org/10.3324/haematol.2025.287934>

©2026 Ferrata Storti Foundation
Published under a CC BY-NC license 

Supplemental methods

Flow cytometry

FACSCelesta (BD Biosciences) and Attune NxT (ThermoFisher) flow cytometers were used with data analyzed in FlowJo (v10.8.1). All samples were washed with FACS buffer or PBS when using live/dead stains.

Antibodies used are listed in **Table S2**.

Cell line culture

All cell lines were maintained in a humidified incubator at 37°C with 5% CO₂. MV-4-11 and K-562 were obtained from the American Type Culture Collection (ATCC) and maintained in Iscove's Modified Dulbecco's Medium (IMDM, Gibco) supplemented with 10% fetal bovine serum (FBS, Hyclone Laboratories). MOLM-13 was maintained in Roswell Park Memorial Institute (RPMI, Gibco) complete with 10% FBS and was originally purchased from the German Collection of Microorganisms and Cell Cultures (DSMZ). Cell lines were transduced with retroviral vectors containing various reporters encoded in pSFG plasmids to enable tracking in experiments. All transduced cell lines were sorted using a BD FACSMelody Cell Sorter and confirmed positive for reporters by flow or by using substrates for enzymes when applicable. HEK293T cells used for viral production were maintained in Dulbecco's Modified Eagle Medium (DMEM, Gibco) complete with 10% FBS and were originally obtained from ATCC. Cell lines were authenticated (Johns Hopkins Genetic Resources Core Facility) and tested for mycoplasma (MycoAlert Detection kit, Lonza) when new cell lines were established after transduction and when stock vials were frozen down.

CD123xCD3 transgene generation

The CD123xCD3 sequence was subcloned into a pMSGV backbone. A sequence encoding a stable marker (full length CD20) was followed by a viral skip sequence (T2A) and a CD123-specific single chain fragment variable (scFv, 26292)¹ conjugated to a CD3-specific scFv derived from the OKT3 clone (Thermo Fisher Scientific) with a serine-glycine linker (GGGGSx3). In-Fusion cloning (Takara Bio) was used to generate a plasmid tagged with nuclear localized mCherry in place of CD20.

Plasmids were amplified in Stellar chemically competent *Escherichia coli* (Takara Bio) and isolated using DNA mini or midi kits (QIAGEN) following the manufacturer's instructions. Sequence fidelity was verified by Sanger sequencing (Johns Hopkins Genetic Resources Core Facility).

Viral production

Research-grade retroviral vector was produced to align with GMP guidelines by the Biopharmaceutical Development Program (Frederick National Laboratory for Cancer Research, Leidos Biomedical Research, Inc).

All vector used was from Lot RD20220810. For CD123xCD3 vectors tagged with nuclear localized mCherry (ENG.NLSmCh) and reporter vectors used to transduce cell lines, replication incompetent RD114 -pseudotyped retroviral vectors were produced in-house using HEK293T cells. Cells were transfected with GeneJuice Transfection Reagent (Sigma-Aldrich) and 10µg of total DNA (3:3:2 of packaging genes, RD114 envelope, and plasmid encoding bispecific). Supernatant containing virus was harvested after 48h, passed through 0.45µm syringe filters, and snap frozen before storing at -80°C.

ENG-T cell production

Peripheral blood mononuclear cells (PBMCs) were isolated from fresh healthy donor blood by layering over Lymphoprep (STEMCELL Technologies) and centrifuging. Buffy coat was collected and washed. PBMCs were frozen in complete RPMI with 10% DMSO and stored long-term in liquid nitrogen. CD4+ and CD8+ cells were isolated from thawed PBMCs using CD4 or CD8 MACS microbeads (Miltenyi Biotec). Briefly, PBMCs were passed through a pre-separation cell strainer (30µm) and incubated with anti-CD4, anti-CD8, or a 1:1 mixture of both microbeads in MACS buffer. Cell suspensions were filtered through lymphocyte selection columns placed in a MACS magnet. Bound cells were washed and then eluted. After purity was confirmed with flow cytometry, selected cells (CD4, CD8, CD4/CD8) and unselected cells were plated on anti-CD3 and anti-CD28 antibody-coated 24-well plates in RPMI complete with 10% FBS and 2mM of GlutaMAX (Gibco). The day following activation, cells were fed with fresh complete medium supplemented with 10ng/mL

recombinant human IL-7 (rhIL-7) and 5ng/mL recombinant human IL-15 (rhIL-15, Biological Resources Branch Preclinical Biorepository, National Cancer Institute). Two days following activation, cells were transduced by plating on virus immobilized to 24-well plates coated with RetroNectin (Takara Bio). Cells were removed from RetroNectin on day 4 after activation and expanded in 24-well tissue culture-treated plates. T cells were split every 2-3 days and refreshed with complete RPMI supplemented with rhIL-7 and rhIL-15.

Transduction efficiency

Transduction efficiency of ENG-T cells was determined by staining for surface CD20. Transduction efficiency of ENG.NLSmCh-T cells was measured by mCherry detection via FACS. Expression was evaluated on day 7 for healthy donor and on day 6 or day 18 for patient-derived ENG-T cells.

Cytotoxicity

CD123+ and CD123-negative target cell lines engineered to express firefly luciferase (ffLuc) were plated with effector cells in a 96-well plate. Cells were incubated for 18h before adding D-luciferin (Thermo Fisher Scientific, 150 μ g/mL). Bioluminescence was measured with a BMG CLARIOstar Plus microplate reader. Cytotoxicity was calculated as the reduction in bioluminescence compared to target-only wells using Microsoft Excel Version 16.94. Patient-derived ENG-T cells were co-cultured 1:1 with autologous AML for 72h. Remaining CD33+ cells were enumerated using fluorophore-conjugated antibodies after staining with a green live/dead stain.

Human AML xenograft mouse model

Female NOD.Cg-Prkdc^{scid}Il2rg^{tm1Wjl}/SzJ (NSG) mice 8-10 weeks old were obtained from an internal colony originally established from the Jackson Laboratory. All protocols were approved by the Johns Hopkins Institutional Animal Care and Use Committee. Mice were injected i.v. with 5e4 MOLM-13.ffLuc cells on day 0 and were treated i.v. on day 7 with unmodified T cells or ENG-T cells produced from healthy whole PBMC, CD4+, CD8+, or CD4+/CD8+ starting material. Before treatment, tumor burden was assessed by bioluminescence imaging and mice were cohorted to eliminate variability. Tumor burden was detected by weekly imaging using an Xenogen IVIS Spectrum. Radiance was quantified

using Living Image v4.7.3. Blood was collected from half of the mice each week via submandibular puncture in EDTA-tubes (RAM Scientific). Mice were monitored clinically for 100 days and sacrificed at humane endpoints.

ENG-T cell production from AML patient biospecimens

ENG.NLSmCh-T cells were produced from biospecimens harvested and banked from five adult patients previously treated at the Johns Hopkins Hospital and consented to the institutional IRB-approved biobanking protocol, J0969. Three of the biospecimens used for *ex vivo* manufacture were PBMCs (patient numbers: 5800, 6034, and 6675) and two were bone marrow mononuclear cells (BMMCs, patient numbers: 4293 and 4316). All patients had disease with a clinical phenotype consistent with AML (**Table S8**). Cells were either unselected or selected for CD4+ and CD8+ cells prior to activation. All PBMC samples were from the day of diagnosis of AML. T cells from patient 4293 were expanded from post-treatment BMMCs while T cells from patient 4316 were expanded from BMMCs isolated from the diagnostic bone marrow sample. Matched autologous AML used in preclinical cytotoxicity assays was obtained from diagnostic bone marrow aspirates. Fold expansion of cells produced from patient samples was determined by manual counting.

Murine peripheral blood (PB) processing

After collection, the volume of PB was recorded. Red cells were lysed with RBC lysis buffer (eBioscience). All samples were blocked with mouse Fc block (BD Biosciences) before antibody staining. Samples were washed and resuspended in the same volume. Samples were run at a set speed and time to acquire a known volume. The acquired volume of sample was used to calculate the volume of blood assayed per mouse.

RNA sequencing

On day 7 after activation, 1e6 unselected or CD4/CD8 pre-selected healthy donor ENG.NLSmCh-T cells were collected. Total RNA was isolated using a RNeasy mini kit (QIAGEN) following the

manufacturer's protocol. RNAseq was performed by Novogene using a non-directional library and a sequencing depth of 20M reads. Enrichment of biologically relevant pathways were identified using Enrichr.^{2,3}

1. Du X, Ho M, Pastan I. New immunotoxins targeting CD123, a stem cell antigen on acute myeloid leukemia cells. *J Immunother*. 2007;30(6):607-613.
2. Chen EY, Tan CM, Kou Y, et al. Enrichr: interactive and collaborative HTML5 gene list enrichment analysis tool. *BMC Bioinformatics*. 2013;14:128.
3. Kuleshov MV, Jones MR, Rouillard AD, et al. Enrichr: a comprehensive gene set enrichment analysis web server 2016 update. *Nucleic Acids Res*. 2016;44(W1):W90-97.

Table S1. FDA-approved engineered T-cell therapies

Product	AKA	Construct	Initial Approval	Manufacturer	Activation	Transduction	Selection	Ref
tisagenlecleucel	tisa-cel, KYMRIAH	α CD19. 41BB. ζ	2017	Novartis	anti-CD3/CD28 antibody-coated microbeads	lentivirus	No	²⁰
axicabtagene ciloleucel	axi-cel, YESCARTA	α CD19. CD28. ζ	2017	Kite Pharma	anti-CD3 antibody and IL-2	retrovirus	No	²¹
brexucabtagene autoleucel	brexu-cel, TECARTUS	α CD19. CD28. ζ	2020	Kite Pharma	anti-CD3 and anti-CD28 antibodies and IL-2	retrovirus	Positive selection of CD4+ and CD8+	^{13,22}
idecabtagene vicleucel	ide-cel, ABECMA	α BCMA. 41BB. ζ	2021	Celgene	anti-CD3 and anti-CD28 antibodies and IL-2	lentivirus	No	^{23,24}
lisocabtagene maraleucel	liso-cel, BREYANZI	α CD19. 41BB. ζ	2021	Celgene and Juno Therapeutics	anti-CD3/CD28 antibody-coated microbeads	lentivirus	Positive selection of CD4+ and CD8+, separately	^{25,26}
ciltacabtagene autoleucel	cilta-cel, CARVYKTI	α BCMA. 41BB. ζ	2022	Janssen Biotech	CD3/CD28- stimulating microbeads and IL-2	lentivirus	Negative selection of pan T cells	^{27,28}
afamitresogene autoleucel	afami-cel, TECELRA	α MAGE- A4 TCR	2024	Adaptimmune	CD3/CD28- stimulating microbeads	lentivirus	No	^{29,30}

Table S2. Antibody list

Antibody	Fluorophore	Reference
T-cell activation		
CD3		Miltenyi: 130-093-387
CD28		BD: 555725
ELISA		
Goat Anti-Mouse IgG, F(ab') ₂ fragment specific		Jackson ImmunoResearch: 115-006-072
Bovine anti-goat HRP		Jackson ImmunoResearch 805-035-180
Purity panel – healthy donor day 0 and all patient-derived cells		
CD3	PerCP-Vio700	Miltenyi: 130-113-132
CD4	APC-Vio770	Miltenyi: 130-113-251
CD8	PE	Miltenyi: 130-113-158
CD33	VioBlue	Miltenyi: 130-111-141
CD123	BB515	BD: 567715
CD20	BV786	BD: 743611
Purity panel – healthy donor day 7		
CD4	PerCP-Cy5.5	BD: 566923
CD8	FITC	BD: 347313
CD33	BV421	BD: 744761
CD123	BV786	BD: 564196
CD20	APC	BD: 559776
Immunophenotype panel		
CD4	BV750	BD: 747176
CD8	BV421	BD: 562428
CCR7	APC	BD: 566762
CD45RA	PE	BD: 555489
LIVE/DEAD		ThermoFisher: L34969
Immunophenotype panel with transduction marker		
CD4	PerCP-Cy5.5	BD: 560650
CD8	BV421	BD: 562428
CCR7	APC	BD: 566762
CD45RA	BV510	BD: 563031
CD20	PE	BD: 555623
Exhaustion panel		
PD-1	Alexa 647	BD: 560838
LAG-3	PE	BD: 565616
TIM-3	BV421	BD: 565562
CD4	BV750	BD: 747176
CD8	APC-Cy7	BD: 557760
LIVE/DEAD		ThermoFisher: L34969
Murine peripheral blood panel		
hCD45	FITC	BD: 555482
hCD20	APC	BD: 559776
hCD33	BV421	BD: 744761

Table S3. Parameters for AML viability curves fit to each stimulation of pre-selected, set ratio ENG-T cells

	CD4	3:1	1:1	1:3	CD8
Stimulation 1					
Best-fit B0 (95% CI)	105.5 (103.9 to 107.0)	105.4 (103.6 to 107.2)	105.3 (102.9 to 107.7)	104.5 (101.8 to 107.2)	104 (99.62 to 108.3)
Best-fit B1 (95% CI)	-32.64 (-36.60 to -28.68)	-53.7 (-58.31 to -49.09)	-72.54 (-78.63 to -66.45)	-83.5 (-90.35 to -76.65)	-90.07 (-101.1 to -79.08)
Best-fit B2 (95% CI)	-5.807 (-7.888 to -3.726)	1.737 (-0.6863 to 4.161)	10.73 (7.526 to 13.93)	16.41 (12.82 to 20.01)	19.88 (14.11 to 25.65)
R ²	0.9843	0.9843	0.9755	0.9702	0.9521
Stimulation 2					
Best-fit B0 (95% CI)	179.5 (137.5 to 221.5)	331.4 (296.5 to 366.2)	394.5 (361.0 to 428.0)	420.4 (387.3 to 453.5)	415.8 (361.8 to 469.8)
Best-fit B1 (95% CI)	-31.11 (-60.69 to -1.535)	-142.5 (-167.0 to -117.9)	-190.4 (-213.9 to -166.8)	-211.1 (-234.3 to -187.8)	-206.8 (-244.8 to -168.8)
Best-fit B2 (95% CI)	-2.304 (-7.355 to 2.747)	15.79 (11.60 to 19.98)	23.63 (19.60 to 27.65)	27.16 (23.19 to 31.14)	26.24 (19.75 to 32.74)
R ²	0.9183	0.9552	0.9628	0.9643	0.9417
Stimulation 3					
Best-fit B0 (95% CI)	397.4 (207.6 to 587.2)	704 (580.6 to 827.5)	1117 (1055 to 1178)	1252 (1170 to 1334)	1173 (1015 to 1330)
Best-fit B1 (95% CI)	-118.8 (-196.8 to -40.86)	-233.7 (-284.4 to -183.0)	-396.6 (-421.8 to -371.5)	-454.8 (-488.5 to -421.2)	-420.4 (-484.9 to -355.8)
Best-fit B2 (95% CI)	10.84 (2.926 to 18.76)	20.46 (15.31 to 25.61)	35.67 (33.12 to 38.23)	41.56 (38.15 to 44.98)	37.96 (31.41 to 44.52)
R ²	0.2922	0.8639	0.9818	0.9696	0.9306
Stimulation 4					
Best-fit B0 (95% CI)	-678.5 (-1080 to -277.2)	233.3 (-467.6 to 934.1)	921.7 (567.9 to 1275)	1562 (1148 to 1977)	2081 (1771 to 2391)
Best-fit B1 (95% CI)	225.7 (109.1 to 342.3)	-24.89 (-228.5 to 178.8)	-218.7 (-321.5 to -115.9)	-402.8 (-523.2 to -282.5)	-547 (-637.1 to -456.9)
Best-fit B2 (95% CI)	-16.16 (-24.58 to -7.734)	0.3576 (-14.35 to 15.07)	13.47 (6.046 to 20.90)	26.32 (17.63 to 35.01)	36.15 (29.64 to 42.65)
R ²	0.1288	0.2097	0.7412	0.7628	0.9303
Stimulation 5					
Best-fit B0 (95% CI)	-1907 (-2509 to -1304)	118.2 (-1718 to 1955)	964.8 (-371.9 to 2302)	3600 (3044 to 4156)	2955 (1783 to 4127)
Best-fit B1 (95% CI)	456.9 (321.3 to 592.4)	4.119 (-409.0 to 417.2)	-176.4 (-477.1 to 124.3)	-763.8 (-889.0 to -638.7)	-612 (-875.7 to -348.3)
Best-fit B2 (95% CI)	-25.9 (-33.50 to -18.31)	-1.027 (-24.18 to 22.13)	8.343 (-8.513 to 25.20)	40.62 (33.61 to 47.63)	31.87 (17.09 to 46.65)
R ²	0.3332	0.05155	0.2843	0.8535	0.688
Stimulation 6					
Best-fit B0 (95% CI)	-2707 (-4512 to -902.4)	214.3 (-2588 to 3017)	2309 (447.9 to 4171)	5371 (4648 to 6095)	2012 (-966.3 to 4991)
Best-fit B1 (95% CI)	527.4 (196.1 to 858.8)	-2.451 (-516.9 to 512.0)	-378.1 (-719.8 to -36.44)	-937.3 (-1070 to -804.4)	-319.8 (-866.5 to 227.0)
Best-fit B2 (95% CI)	-24.73 (-39.90 to -9.554)	-0.997 (-24.55 to 22.56)	15.66 (0.009233 to 31.30)	40.95 (34.86 to 47.03)	12.9 (-12.14 to 37.93)
R ²	0.1637	0.1325	0.4494	0.9	0.3476
Stimulation 7					
Best-fit B0 (95% CI)	-3934 (-7574 to -293.7)	1958 (-2424 to 6339)	6047 (4398 to 7697)	5691 (5075 to 6306)	163.2 (-2322 to 2648)
Best-fit B1 (95% CI)	641.8 (77.37 to 1206)	-266.8 (-946.2 to 412.5)	-894 (-1150 to -638.2)	-827.8 (-923.3 to -732.3)	20.28 (-365.1 to 405.6)

Best-fit B2 (95% CI)	-25.47 (-47.31 to -3.625)	9.297 (-17.00 to 35.59)	33.14 (23.24 to 43.03)	30.17 (26.47 to 33.87)	-2.113 (-17.03 to 12.80)
R²	0.1151	0.133	0.7175	0.9646	0.541

Stimulation 8

Best-fit B0 (95% CI)	-3337 (-7831 to 1157)	3899 (-664.1 to 8462)	7093 (5476 to 8710)	-421.7 (-1699 to 855.5)	1533 (484.9 to 2582)
Best-fit B1 (95% CI)	486.5 (-116.7 to 1090)	-481.1 (-1094 to 131.3)	-905 (-1122 to -687.9)	109.6 (-61.83 to 281.0)	-202.4 (-343.1 to -61.67)
Best-fit B2 (95% CI)	-17.2 (-37.42 to 3.014)	14.96 (-5.563 to 35.49)	28.94 (21.66 to 36.21)	-5.155 (-10.90 to 0.5905)	7.139 (2.422 to 11.86)
R²	0.2183	0.3021	0.8422	0.8955	0.5559

Stimulation 9

Best-fit B0 (95% CI)	-5197 (-12831 to 2437)	4672 (-2111 to 11455)	10149 (8202 to 12096)	1247 (-136.8 to 2630)	-1141 (-2127 to -154.3)
Best-fit B1 (95% CI)	647.3 (-255.9 to 1551)	-516.7 (-1319 to 285.9)	-1154 (-1384 to -923.2)	-97.49 (-261.2 to 66.20)	140.7 (23.95 to 257.4)
Best-fit B2 (95% CI)	-19.76 (-46.46 to 6.930)	14.38 (-9.335 to 38.10)	32.82 (26.01 to 39.63)	1.63 (-3.207 to 6.468)	-3.947 (-7.396 to -0.4982)
R²	0.1015	0.1968	0.8699	0.9171	0.5053

Stimulation 10

Best-fit B0 (95% CI)	-5344 (-13664 to 2976)	9925 (6689 to 13161)	4655 (1389 to 7921)	2599 (85.37 to 5112)	772.4 (417.7 to 1127)
Best-fit B1 (95% CI)	587.9 (-292.4 to 1468)	-1001 (-1343 to -658.3)	-439.3 (-784.8 to -93.81)	-271.6 (-537.5 to -5.675)	-72.46 (-110.0 to -34.93)
Best-fit B2 (95% CI)	-15.86 (-39.13 to 7.401)	25.25 (16.21 to 34.30)	10.35 (1.222 to 19.48)	7.379 (0.3506 to 14.41)	1.95 (0.9577 to 2.941)
R²	0.05457	0.7956	0.7991	0.1726	0.3763

Stimulation 11

Best-fit B0 (95% CI)	-1265 (-14261 to 11730)	9627 (6506 to 12747)	523.6 (-2148 to 3195)	-2139 (-3544 to -734.0)	58.15 (-1855 to 1972)
Best-fit B1 (95% CI)	140.5 (-1103 to 1384)	-870.6 (-1169 to -572.1)	-5.581 (-261.2 to 250.0)	198.3 (63.87 to 332.7)	2.335 (-180.7 to 185.4)
Best-fit B2 (95% CI)	-3.614 (-33.33 to 26.10)	19.71 (12.58 to 26.85)	-0.7762 (-6.885 to 5.333)	-4.317 (-7.530 to -1.104)	-0.006003 (-4.382 to 4.370)
R²	0.01882	0.8624	0.8486	0.8167	0.04804

Where B0, B1, and B2 are parameters of the second order polynomial equation: $Y = B0 + B1*X + B2*X^2$

Table S4. Select Reactome 2022 Terms: Upregulated in CD4/CD8-selected vs. unselected ENG-T

Term	Overlap	P-value	Adjusted P-value	Odds Ratio	Combined Score	Genes
LGI-ADAM Interactions R-HSA-5682910	2/14	0.009	0.589	16.3	77.5	LGI4; ADAM11
Constitutive Signaling By NOTCH1 HD Domain Mutants R-HSA-2691232	2/15	0.010	0.589	15.1	69.4	NEURL1B; MIB2
Ion Transport By P-type ATPases R-HSA-936837	2/53	0.014	0.232	12.0	51.5	FXYD7; ATP2C2
Biological Oxidations R-HSA-211859	4/218	0.010	0.357	5.0	23.2	GSTM2; EPHX1; DPEP2; PAPSS2
RUNX3 Regulates WNT Signaling R-HSA-8951430	1/8	0.030	0.357	37.4	130.8	TCF7L2
Transport Of Vitamins, Nucleosides, And Related Molecules R-HSA-425397	2/43	0.002	0.154	30.4	182.9	SLC35D2; SLC29A4
TP53 Regulates Transcription Of Cell Death Genes R-HSA-5633008	2/44	0.003	0.154	29.6	177.2	BCL6; TP53INP1

Table S5. Select Reactome 2022 Terms: Downregulated in CD4/CD8-selected vs. unselected ENG-T

Term	Overlap	P-value	Adjusted P-value	Odds Ratio	Combined Score	Genes
Interleukin-10 Signaling R-HSA-6783783	4/45	0.000	0.038	19.4	181.1	CCR1; CCL22; CD80; LIF
Chemokine Receptors Bind Chemokines R-HSA-380108	4/56	0.000	0.044	15.3	129.6	CCR1; CXCL9; CCL22; CXCR1
Signaling By Interleukins R-HSA-449147	9/453	0.001	0.086	4.2	30.8	LYN; CCR1; CDKN1A; ITGAM; CCL22; ANXA2; IFNG; CD80; LIF
Interleukin-4 And Interleukin-13 Signaling R-HSA-6785807	4/107	0.002	0.195	7.7	46.5	CDKN1A; ITGAM; CCL22; LIF
Glycosphingolipid Metabolism R-HSA-1660662	2/45	0.005	0.178	21.5	115.9	B3GALNT1; ARSB
GPCR Downstream Signaling R-HSA-388396	5/619	0.012	0.178	3.9	17.3	CXCL9; CXCR1; TRPC3; RGS16; RGS6
Cell Cycle R-HSA-1640170	9/654	0.000	0.040	5.4	48.7	LYN; GINS2; FEN1; CDKN1A; CENPW; MCM10; CLSPN; POLR2L; SPC25
Cytokine Signaling In Immune System R-HSA-1280215	8/702	0.001	0.076	4.4	30.0	LYN; CCR1; CDKN1A; CCL22; CD40LG; ANXA2; IFNG; LIF
RNA Polymerase III Chain Elongation R-HSA-73780	2/17	0.001	0.076	46.6	316.2	POLR3K; POLR2L
Pyroptosis R-HSA-5620971	2/26	0.003	0.094	29.1	172.7	GZMB; CYCS

Table S6. Select GO Biological Processes 2023: Upregulated in CD4/CD8-selected vs. unselected ENG-T

Term	Overlap	P-value	Adjusted P-value	Odds Ratio	Combined Score	Genes
Positive Regulation Of Synaptic Transmission (GO:0050806)	5/77	0.001	0.187	6.9	46.6	NLGN2; DLG4; NOL3; BAIAP3; NFATC4
Release Of Sequestered Calcium Ion Into Cytosol By Sarcoplasmic Reticulum (GO:0014808)	2/6	0.002	0.187	49.0	318.2	RYR1; NOL3
Calcium Ion Transmembrane Import Into Cytosol (GO:0097553)	5/83	0.002	0.187	6.4	40.9	RYR1; CACNA1I; JPH2; PLCH2; CACNA1F
Regulation Of Sodium Ion Transmembrane Transporter Activity (GO:2000649)	2/37	0.007	0.278	17.5	87.2	FXYD7; FGF11
Lipid Modification (GO:0030258)	2/42	0.009	0.278	15.3	72.5	PLPPR2; EPHX2
Negative Regulation Of Lipid Kinase Activity (GO:0090219)	1/7	0.023	0.278	50.3	189.3	PIK3IP1
T-helper 17 Cell Lineage Commitment (GO:0072540)	1/7	0.023	0.278	50.3	189.3	LY9
Unsaturated Fatty Acid Metabolic Process (GO:0033559)	2/49	0.015	0.282	11.3	47.1	GSTM2; EPHX1
Icosanoid Metabolic Process (GO:0006690)	2/52	0.017	0.282	10.6	43.1	EPHX1; DPEP2
Purine Ribonucleotide Biosynthetic Process (GO:0009152)	2/55	0.019	0.282	10.0	39.6	ADCY4; PAPSS2
Positive Regulation Of Lipid Localization (GO:1905954)	2/10	0.000	0.019	208.0	1,982.0	LRP1; HILPDA
Calcium Ion Transmembrane Import Into Cytosol (GO:0097553)	3/83	0.000	0.022	32.4	282.1	RYR1; CACNA1I; JPH2
Monoatomic Cation Homeostasis (GO:0055080)	2/77	0.004	0.088	22.1	119.6	JPH2; TMPRSS6
Regulation Of Metallopeptidase Activity (GO:1905048)	1/6	0.008	0.088	159.8	775.9	LRP1
Lymphocyte Apoptotic Process (GO:0070227)	1/7	0.009	0.088	133.1	626.1	EBF4

Table S7. Select GO Biological Processes 2023: Downregulated in CD4/CD8-selected vs. unselected ENG-T

Term	Overlap	P-value	Adjusted P-value	Odds Ratio	Combined Score	Genes
Positive Regulation Of Peptidyl-Tyrosine Phosphorylation (GO:0050731)	6/130	0.000	0.064	9.8	94.8	LYN; IFNG; CD80; LIF; OSM; LRP8
Lymphocyte Proliferation (GO:0046651)	3/38	0.001	0.111	16.9	116.3	CD40LG; CTPS1; MS4A1
B Cell Receptor Signaling Pathway (GO:0050853)	3/46	0.000	0.058	33.1	291.0	IGHG2; IGHA1; MS4A1
Regulation Of T Cell Mediated Immunity (GO:0002709)	2/11	0.000	0.058	103.1	847.5	FUT7; CD80

Table S8. Surface marker phenotype of primary AML samples reported by the Johns Hopkins Hospital clinical hematopathology lab

6675	CD38, variable HLA-DR, CD117, CD123 , dim CD11b, CD64, bright CD33 and bright CD13 and completely lack CD34, and are negative for CD19, CD7, CD3 and other T cell markers
6034	bright CD13 and CD34, moderate CD38, CD117, CD123 and HLA-DR with partial CD2, CD4 , CD7, CD64 and CD200. There is substantial loss of CD33
5800	express CD34, partial variable CD117, CD38, partial dim CD123 , bright CD13, variable CD33, and partial CD64, and with partial loss of HLA-DR
4293	Intermediate intensity CD45, negative for CD34, with expression of CD117 (dim), CD123 (dim) , HLADR, CD64, CD33, and CD4 . Partial dim CD7, CD15, and CD56.
4316	Variable CD34 with expression of CD117, HLADR, CD13, CD33, and CD123 and loss of CD38

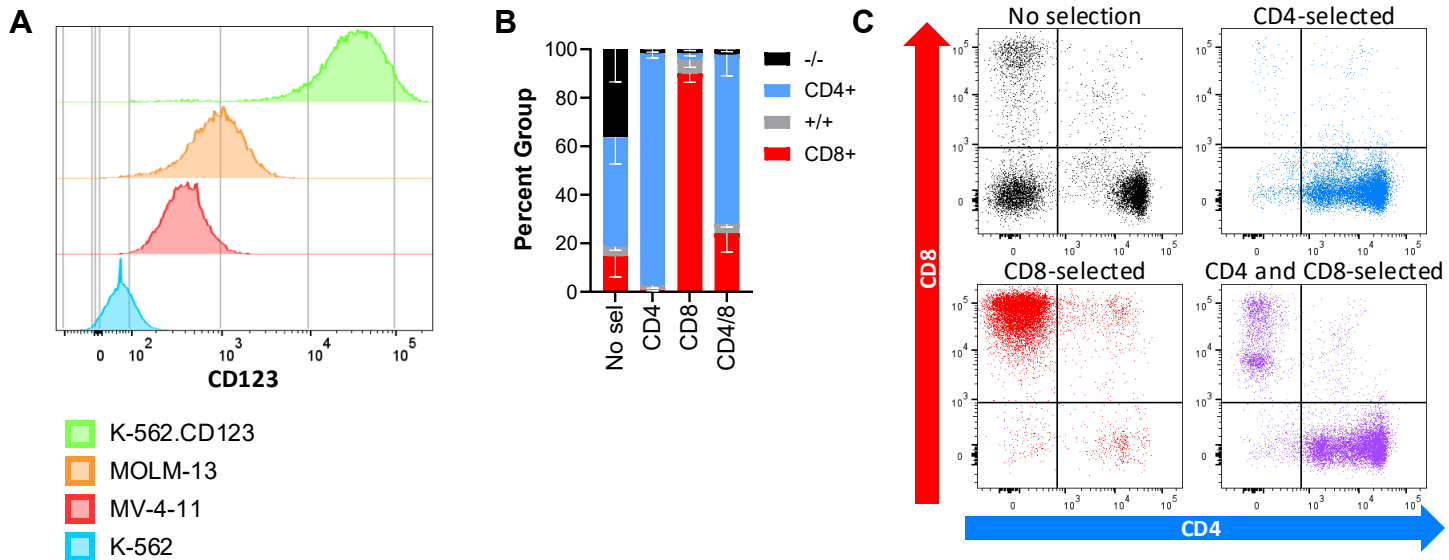
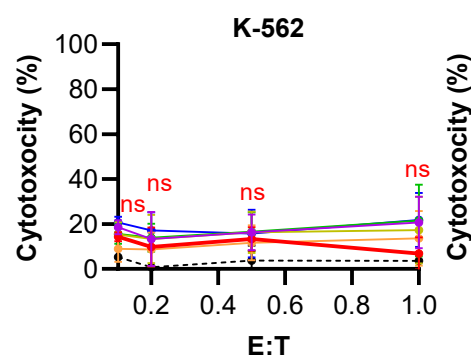


Figure S1. CD123 expression varies between model cell lines and PBMC T-cell selections result in pure populations. (A) Representative anti-CD123 antibody staining of K-562, MOLM-13, MV-4-11, and K-562 engineered to express CD123 (K-562.CD123). **(B)** Quantification of CD4+ and CD8+ population distributions following selection before activation on day 0. N = 4-6 unique T-cell donors. **(C)** Representative flow plots of selections from one donor.

A



B

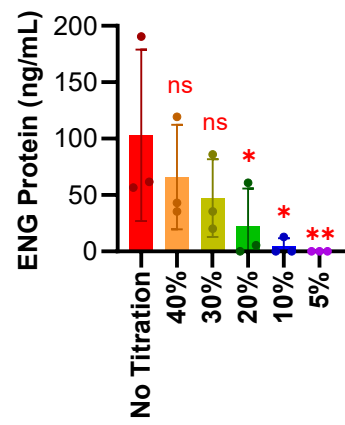


Figure S2. Antigen-specific anti-tumor activity is independent of transduction efficiency. (A) Transduced CD4/CD8-selected T cells were titrated with identically cultured autologous unmodified CD4/CD8-selected T cells to achieve the desired ENG% (0 to 64%). T cells were co-cultured with either K-562 (CD123-negative) or K-562.CD123, both engineered to express firefly luciferase, for 18-hours at indicated effector-to-target (E:T) ratios. Cytotoxicity was determined by calculating the reduction in bioluminescent signal compared to target cells cultured without T cells. Differences between selection groups at each E:T were assessed by three-way ANOVA (donor, transduction efficiency, E:T) with Tukey tests for multiple comparisons using R. N = 3 independent experiments, 2 unique T-cell donors. (B) CD123xCD3 secreted by 1e6 titrated cells plated in 2 mL of cytokine supplemented media measured after 24 hours by ELISA. Two-way ANOVA (donor and transduction efficiency) with Tukey correction was used to compare secreted protein amounts to no titration condition. N = 3 unique T-cell donors. For both (A) and (B), titrated cells were allowed to incubate in cytokine-supplemented media after mixing for at least 24 hours before use in experiments. ns = not significant vs. No Titration, *p < 0.05, **p ≤ 0.01. Transduction efficiency ranged from 55 to 64% in the No Titration condition.

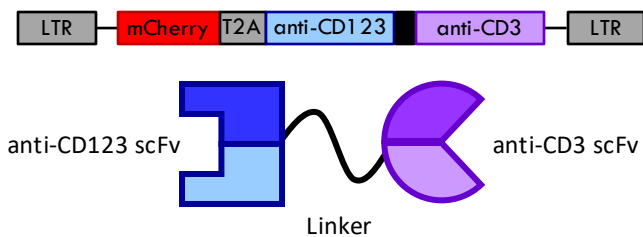
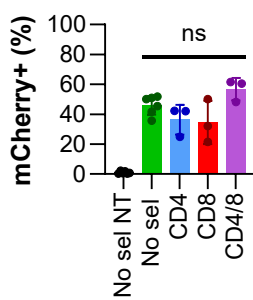
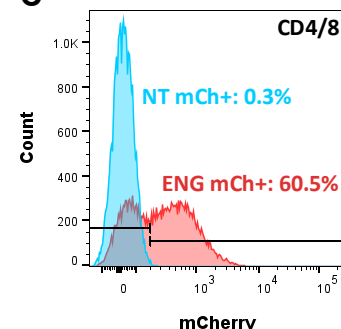
A**B****C**

Figure S3. T cells are effectively modified with a NLS-mCherry tagged ENG construct. (A) ENG-T cells were modified with viral vectors containing mCherry tagged with a nuclear localization sequence (NLS-mCherry) and our CD123xCD3 bispecific separated by a T2A sequence. **(B)** Transduction efficiency was evaluated by flow cytometry and detection of mCherry. Two-way ANOVA (donor and selection) with Tukey correction was used to compare transduction efficiency. N = 3-6 unique T-cell donors. **(C)** Representative histogram of mCherry (mCh) positivity after transduction of CD4/8 pre-selected T cells. No sel = no selection, NT = non-transduced, CD4/8 = CD4 and CD8-selected.

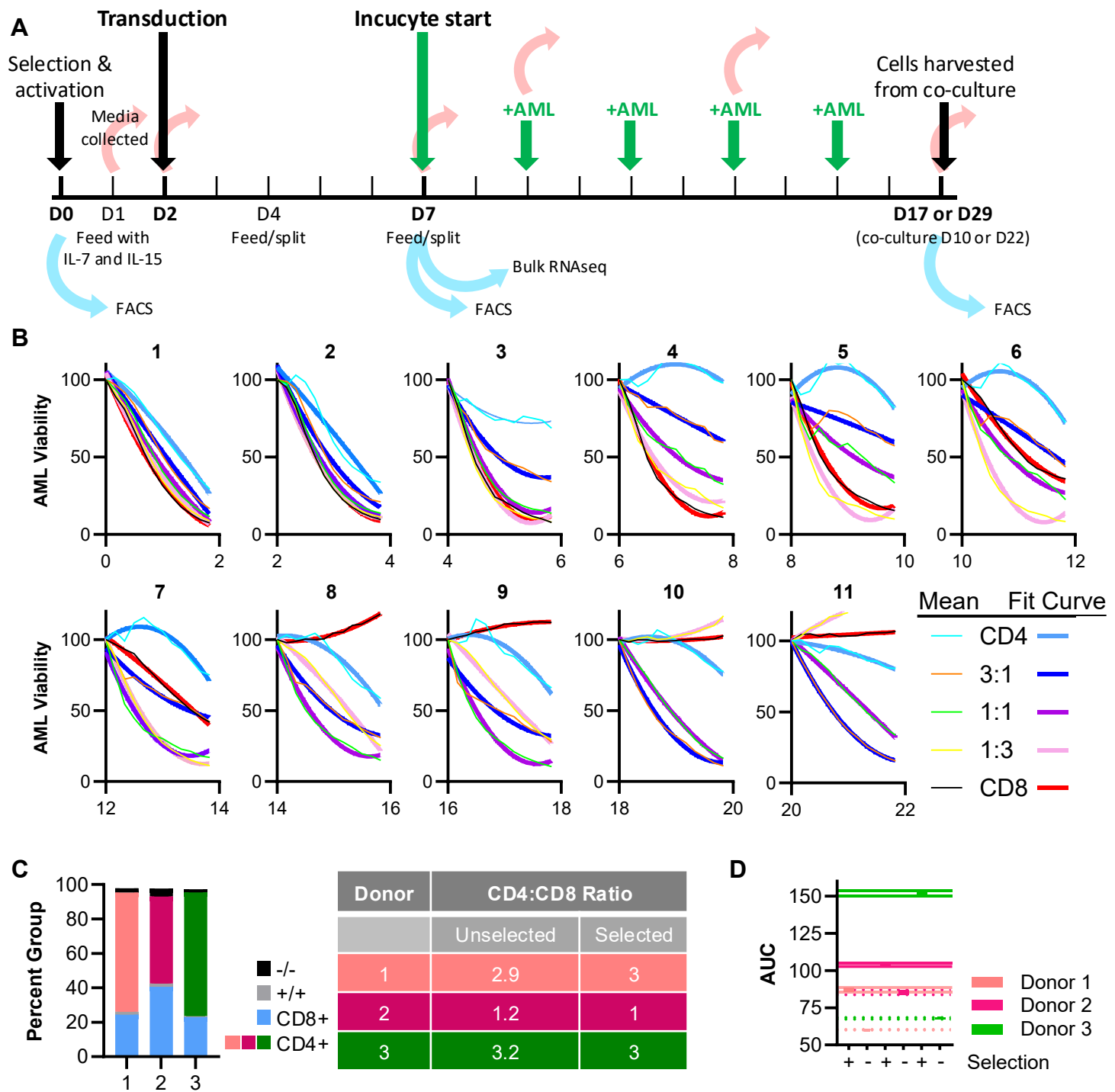


Figure S4. Pre-selection and higher CD4:CD8 ratio improve durable ENG-T cell function. (A) Experimental timeline and analytic schematic for serial stimulation, media harvest, FACS time points, and bulk RNAseq completed during manufacture and co-culture of ENG.NLSmCh-T cells with MOLM-13.NLSGFP. Cells were tracked in a 10- or 22-day serial stimulation assay (day 7 to 17 or 29 post-activation), with fresh target cells added every two days. (B) AML viability is calculated as the average number of green objects counted per image, as a percentage of the total number of green objects recorded at the initiation of each stimulation. AML viability recorded over 11 stimulations and 22 total days in culture with ENG-T cell products with variable CD4:CD8 ratios, as indicated. AML viability curve comparisons were visualized by fitting quadratic curves to each stimulation. 4 images per well, 3 wells per donor and 3 unique T cell donors measured per condition. (C) T-cell composition of unselected ENG-T cell products per donor. (D) Area under the curve (AUC) calculated for T-cell counts and depicted as 95% confidence interval bound for each condition. Dotted: no selection, Solid: Selection.

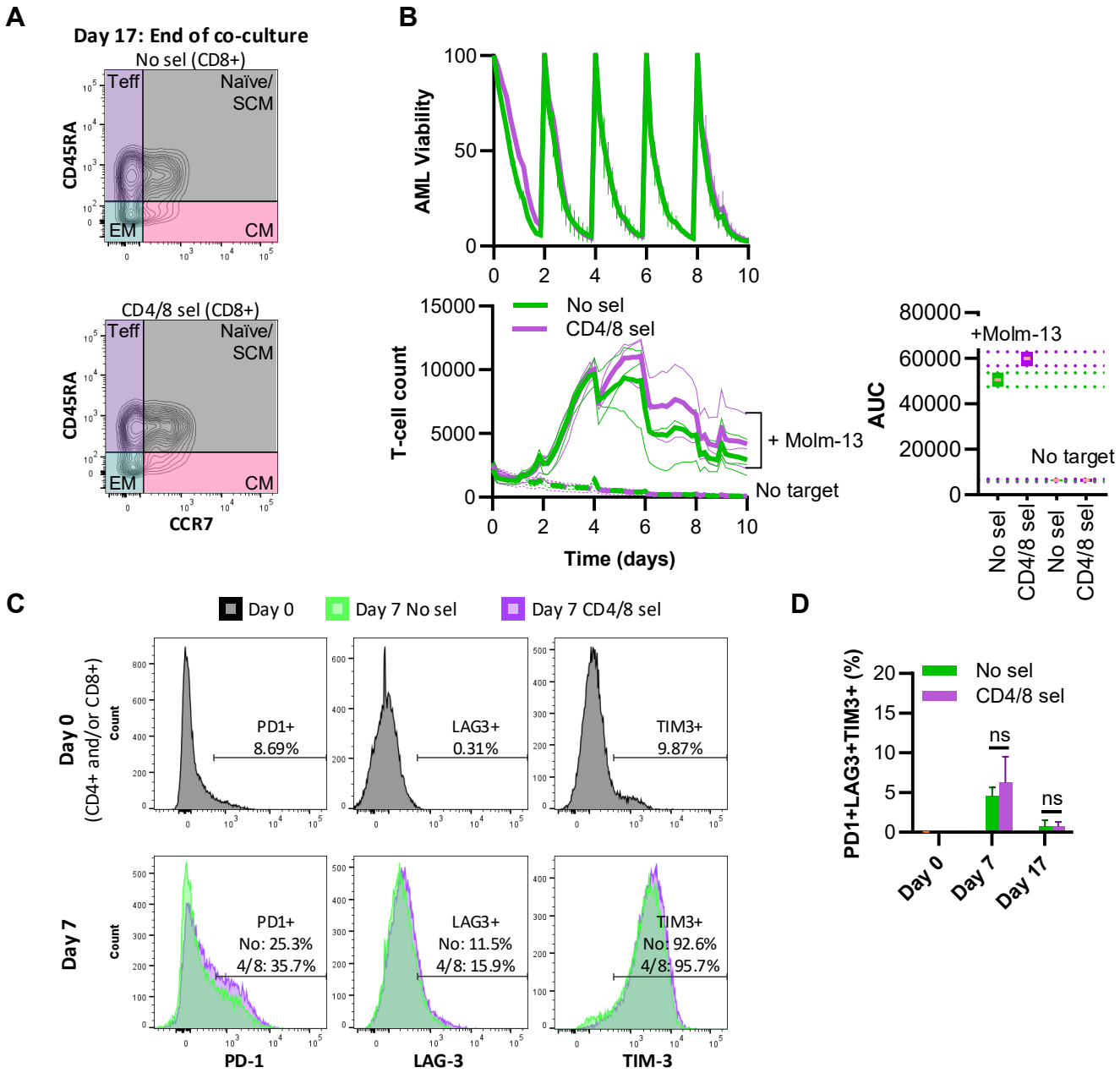


Figure S5. Unselected and CD4/CD8-selected ENG-T cells functional differences not explained by differential expression of exhaustion associated receptors. (A) Representative flow cytometry plots used to define T-cell immunophenotypic subsets of unselected and CD4/CD8-selected ENG.NLSmCh-T cells. (B) ENG-T cells and MOLM-13 marked with NLS-mCherry and NLS-GFP, respectively were co-cultured in an Incucyte S3 live cell imaging system at an initial effector-to-target ratio of 1:1 per well. Cells were tracked in a 10-day serial stimulation assay (day 7 to 17 post-activation), with fresh target cells added every two days. T cells per image were quantified (thick lines = means, thin lines = individual donors) and cytotoxicity was determined by measurement of target cells per image. AML viability is represented as the average number of green objects counted per image, as a percentage of the total number of green objects recorded after re-stimulation. T-cell count is representative of the average number of red objects counted per image. 4 images per well, 6 wells per donor, 3 independent T-cell donors. Area under the curve (AUC) calculated for T-cell counts and depicted as 95% confidence interval for each condition. (C) Representative flow cytometry histograms showing PD-1, LAG-3, and TIM-3 surface expression on T cells before activation on day 0 and surface expression on ENG.NLSmCh-T cells following 7 days of culture. No sel = no selection, CD4/8 = CD4 and CD8-selected. (D) Exhausted cell percentages were measured before and after serial stimulation (D7 vs. D17). Statistical comparison was completed using two-way ANOVA (donor and selection).

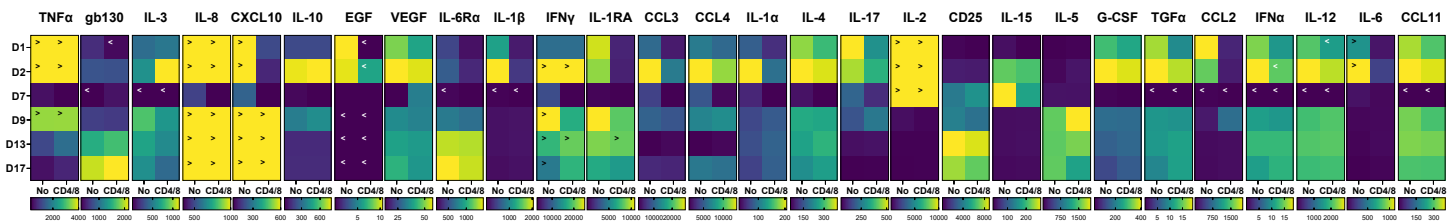


Figure S6. The manufacturing environment of unselected and selected ENG-T cells differs only in the initial days of culture. A panel of cytokines were measured in the supernatant of unselected or CD4/CD8-selected ENG.NLSmCh-T cells during manufacture (day 1, 2, and 7) and serial stimulation (day 9, 13, 17) using a Luminex multiplex assay. A greater-than sign indicates at least one sample above the limit of detection, a less-than sign indicates at least one sample below the limit of detection. Heatmap scale differs for each analyte tested and is indicated below each map. N = 3 unique T-cell donors. No sel = no selection, CD4/8 = CD4 and CD8-selected.

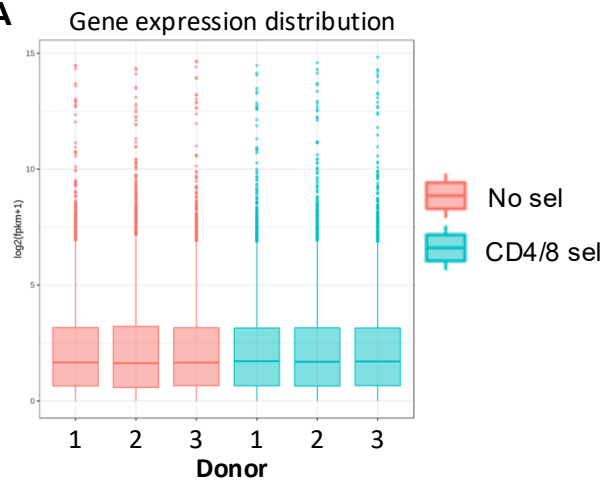
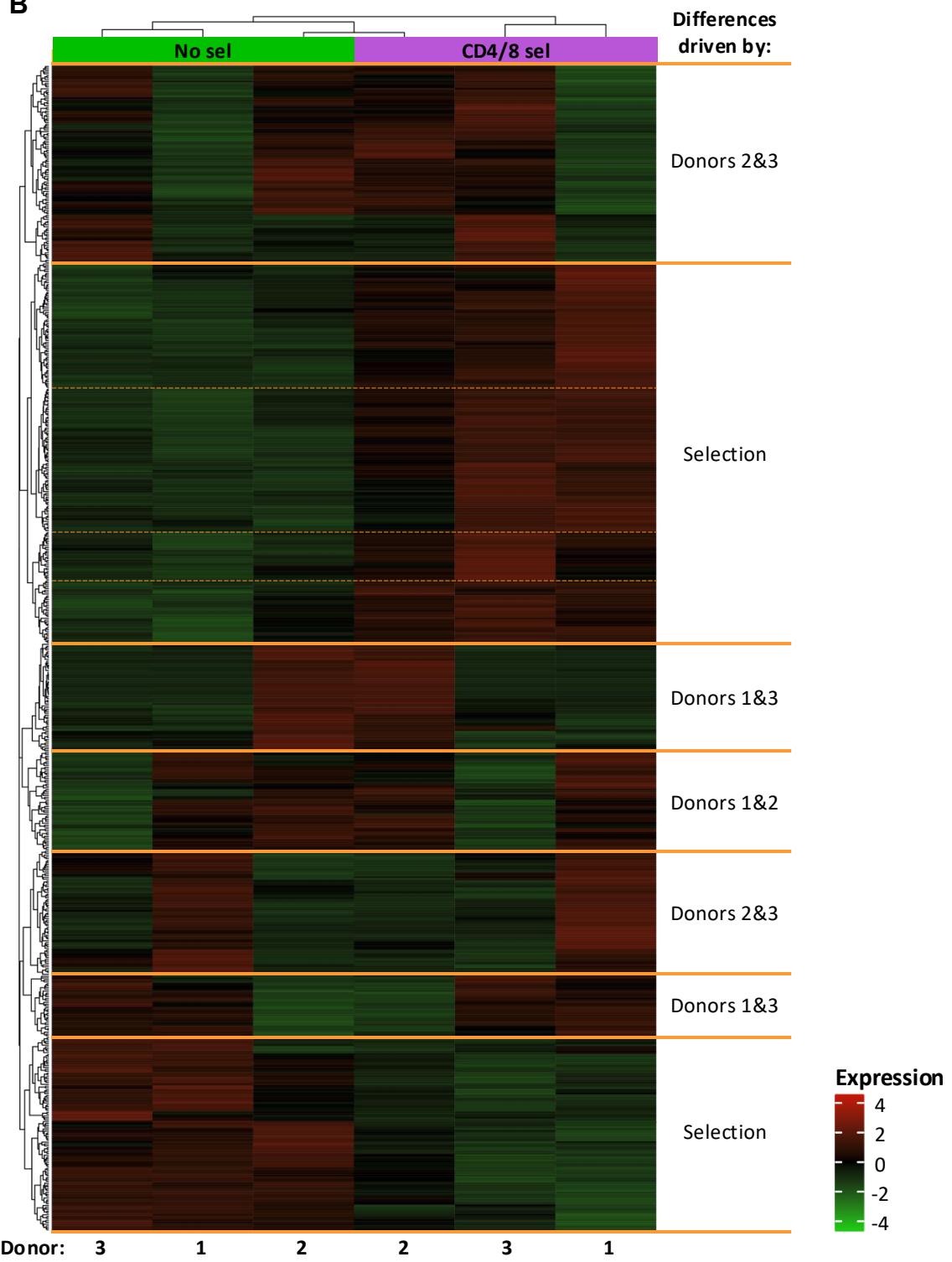
A

Figure S7. CD4/CD8-selection alters the transcriptional profile of ENG-T cells. RNA was extracted from unselected and CD4/CD8-selected ENG.NLSmCh-T cells frozen on day 7 of manufacture. Transcription profiles were assessed by bulk RNAseq. **(A)** Levels of total gene expression were calculated for each selection group and donor. **(B)** Clustering of ENG-T cells using $\log_2(\text{FPKM}+1)$ and normalized expression of transcripts. Major groups of upregulated or downregulated transcripts are separated by orange lines and were defined by the apparent drivers of each cluster. Clusters driven by selection are also reported in **Figure 6A** and were further broken down into subcluster gene sets, indicated by dashed orange lines, for Enrichr analysis. $N = 3$ unique T-cell donors. No sel = no selection, CD4/8 = CD4 and CD8-selected.

B

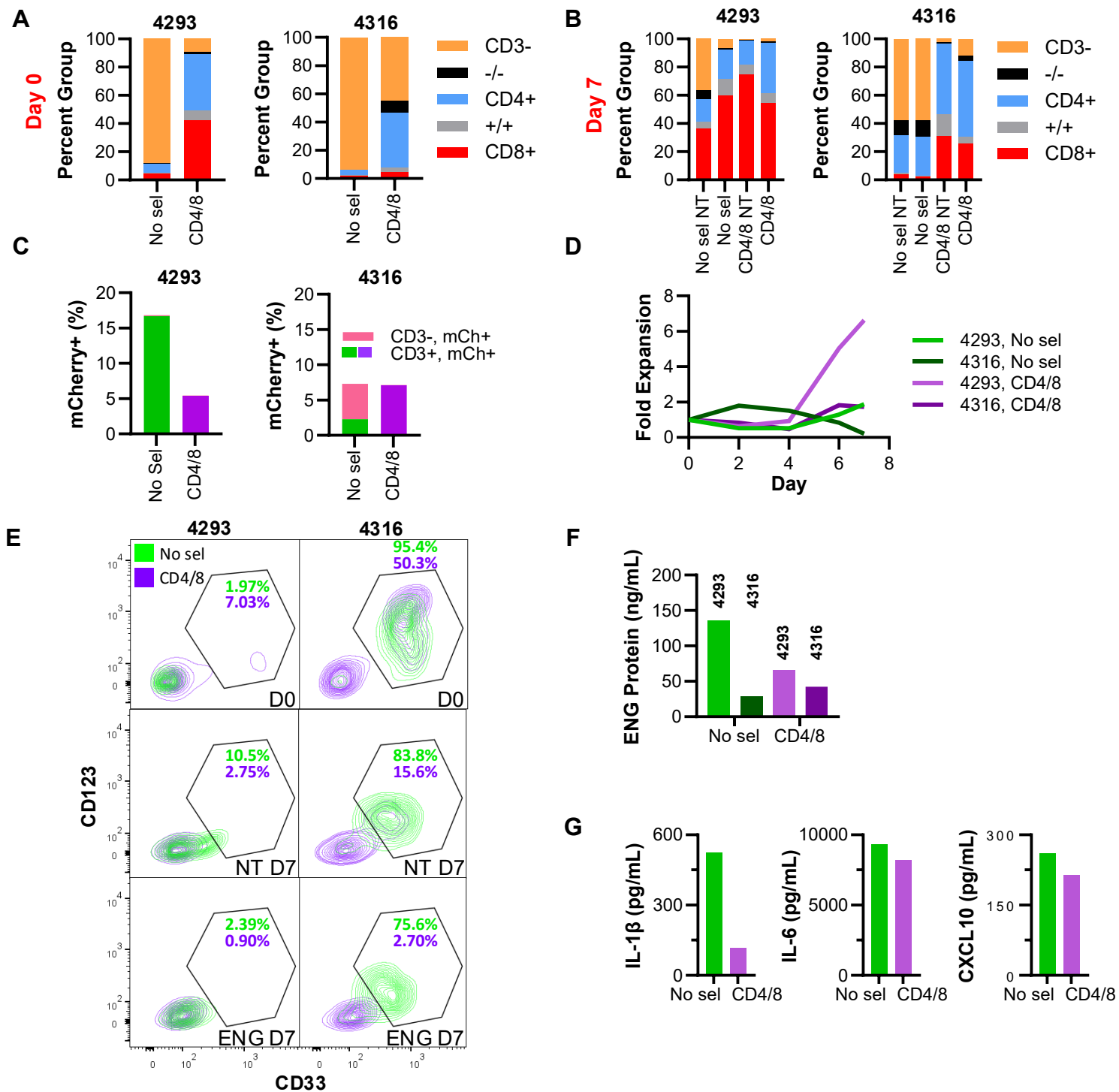


Figure S8. CD4/CD8-selected ENG-T cells produced from patient-derived material have decreased CD3-negative contamination and increased expansion. ENG-T cells were produced from banked bone marrow aspirates from two patients treated at the Johns Hopkins Hospital. **(A)** T cells from patient 4293 and patient 4316 were activated on day 0 either without or after CD4/CD8-selection. CD3+, CD4+, and CD8+ populations were detected using flow cytometry. **(B)** CD3-negative contamination was evaluated on day 7 post-activation using flow cytometry. **(C)** Unselected and selected cells were transduced with an NLS-mCherry tagged ENG vector and expression of mCherry was detected on day 6 post-activation using flow cytometry. **(D)** Expansion of unselected and selected products was evaluated by manual counting. **(E)** The presence of AML (CD123+CD33+) was detected in the material used for unselected and CD4/CD8-selected ENG-T cell manufacture (day 0, D0), in non-transduced expanded T cells, and in expanded ENG-T cell products. Expanded products were evaluated on day 7 (D7) after activation. CD123 and CD33 staining was assessed by flow cytometry. **(F)** Production of CD123xCD3 was confirmed in the expansion media of transduced cell products by ELISA. **(G)** The presence of IL-1 β , IL-6, and CXCL10 were detected in the T-cell expansion media of sample 4293 on the day following activation. Protein concentrations were determined by ELISA. No sel = no selection, CD4/8 = CD4 and CD8-selected.

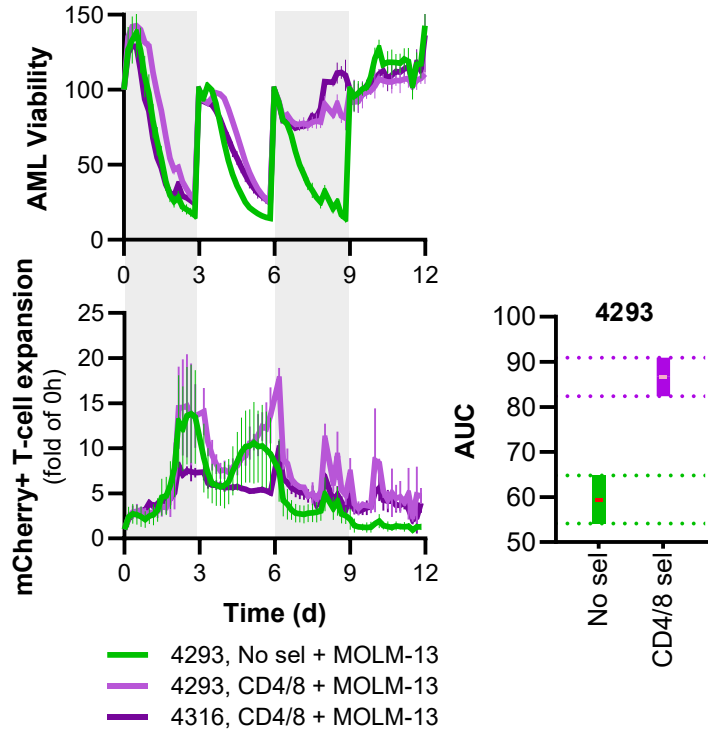
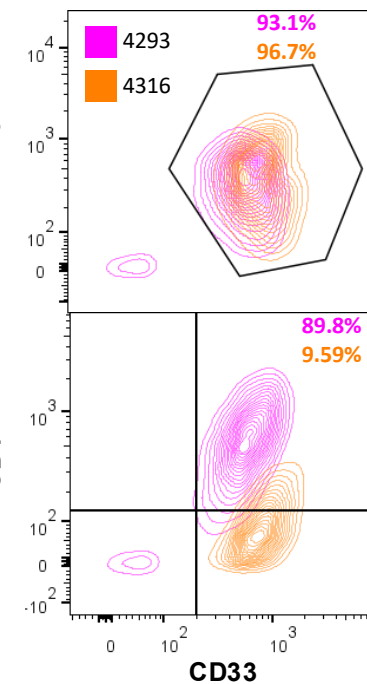
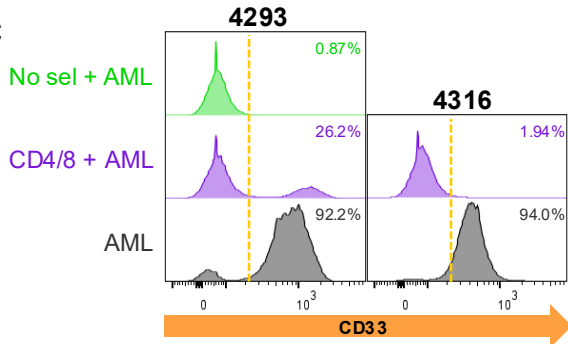
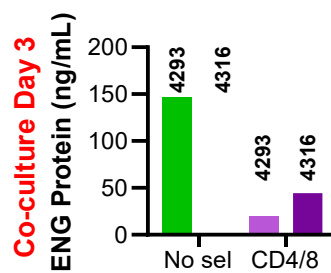
A**B****C****D**

Figure S9. ENG-T cells engineered from patient samples kill AML blasts. (A) ENG-T cell products with effective expansion were plated 1:1 with MOLM-13.NLSGFP in an Incucyte S3 live cell imaging system. T cells were restimulated with more MOLM-13.NLSGFP every 3 days for 12 days (d). AML viability was calculated as the percentage of green objects remaining after each re-stimulation. T-cell expansion was tracked by evaluating the fold change of red objects compared to time 0. For each donor, 3 wells were plated and 4 images were gathered per well. 95% confidence interval for calculated Area Under the Curve (AUC) of matched donor T-cell expansion. (B) Expression of CD33, CD123, and CD4 in AML samples from patient 4293 and 4316, determined by flow cytometry. (C) ENG-T cell products were plated at a 1:1 ratio with autologous AML. Viable CD33+ cells were evaluated after 72h by flow cytometry. (D) The presence of CD123xCD3 molecules was detected in the media of ENG-T and autologous AML co-cultures using ELISA. No sel = no selection, CD4/8 = CD4 and CD8-selected, NT = non-transduced.